applied sciences

MDPI

Article

Performance Analysis and Sensor-Target Geometry Optimization for TOA and TDOA-Based Hybrid Source Localization Method

Guoning Ma, Zhijiang Huang, Ming Wang, Zhengyu Ji, Xianglu Li, Bo Shen and Jie Tian *

Institute of Electronic Engineering, China Academy of Engineering Physics, Mianyang 621999, China
* Correspondence: tianjie@caep.cn

Abstract: Currently, the performance analysis of positioning algorithms and optimization of ground station deployment schemes are predominantly based on pure TOA or TDOA measurement information, and the relevant theoretical analysis is primarily the geometric analysis of optimal station deployment for fixed point targets, with few placement ranges and amount of station constraints. In practice, however, there are typically several measurements from TOA and TDOA stations, with a focus on positioning precision within a certain region or line trajectory, as well as the necessity for constraints on the ground station placement range. This paper proposes an efficient method for hybrid source localization using TOA and TDOA measurement information, establishes a mathematical model for hybrid source localization based on TOA and TDOA measurement information, derives and simulates the Gauss–Newton iterative localization algorithm with the least squares criterion, and performs a theoretical analysis of the least squares error and CRLB boundary to improve the accuracy of target localization in the aforementioned scenarios. Taking the average CRLB value of target line trajectory positioning error as the objective function, the ground station placement scheme of TOA- and TDOA-receiving sensors is optimized by utilizing a Genetic Algorithm with strong global optimization capability under the constraints of station placement range and station quantities, and a station placement geometry with better performance than typical station placement is obtained. Meanwhile, we summarize the general placement principles for TOA and TDOA hybrid source localization of target line trajectories.

Keywords: TOA; TDOA; hybrid source localization; least-square algorithm; Cramer Rao Low Bound (CRLB); Genetic Algorithm (GA)

Citation: Ma, G.; Huang, Z.; Wang, M.; Ji, Z.; Li, X.; Shen, B.; Tian, J. Performance Analysis and Sensor-Target Geometry Optimization for TOA and TDOA-Based Hybrid Source Localization Method. *Appl. Sci.* **2022**, *12*, 12977. https://doi.org/10.3390/app122412977

Academic Editor: Vincent A. Cicirello

Received: 4 November 2022
Accepted: 14 December 2022
Published: 17 December 2022

1. Introduction

The explosive growth of fifth-generation (5G) wireless communications will introduce a large number of new technological scenarios with higher requirements for location-based services [1], precise target localization techniques are becoming increasingly important in the application of radar [2], sonar [3], and wireless sensor networks [4] in 5G. At the same time, in order to improve the utility of mobile navigation scenarios, there is a need not only to provide continuous and comprehensive area coverage for users and seamless and stable indoor and outdoor LBS, but also to provide new ideas by organically synchronizing multiple technologies through public mobile communication systems using convergent positioning [4].

Methods of localization based on communication infrastructure are classified into two types: direct and indirect localization. The essential premise of the direct localization technique is to establish the maximum likelihood (ML) function of the user's location with relevant information and to provide an iterative location estimation of the user [5,6]. The direct method is more accurate, but it relies on the processing of a large amount of data, leading to a higher computational complexity [7–9]. The majority of indirect localization techniques are based on distance measuring. The server at the ground station determines the position of the mobile user by calculating the distance measurement results [10]. In this procedure, direct LOS paths in space are typically employed to measure relevant physical parameters, such as TOA (time of arrival), TDOA (time difference of arrival), AOA (angle of arrival), FDOA (frequency difference of arrival), RSS (received signal strength), etc. Due to their greater accuracy, TOA and TDOA approaches have garnered the most attention, and the corresponding location calculation and performance analysis methods have been intensively investigated [11–16]. For instance, to simplify the TDOA equations, [11] utilized elliptical coordinates and asymptotes to determine the target's position in far-field situations. By linearizing the approximate ML estimation, [12] suggested a closed-form solution form for the TOA and TDOA localization methods. In [13], the authors examined closed-form solution algorithms and iterative algorithms for four localization methods, as well as a hybrid source localization algorithm based on TOA and AOA. Methods for TDOA localization based on multidimensional scaling and convex optimization have been proposed in [14,15]. Ref. [16] developed a ML approximation for the closed-form solution of AOA under low noise conditions. Maximum Likelihood Estimators utilizing Gauss-Newton or quasi-Newton iterations were developed in [17] to localize a moving target by time delay and Doppler frequency shift using sensors in motion, a structured total least squares method with hybrid TDOA-AOA measurements was developed in [18] to reduce estimation bias, and an algebraic solution using TDOA and FDOA measurements to determine the location and velocity of moving sources was developed in [19] and the method suffers from no initialization and local convergence problems.

In addition to the measurement precision of physical quantities and algorithm performance, the geometric position of the measurement sensor in relation to the target is a significant factor influencing localization accuracy. For two-dimensional TOA and TDOA measurement and localization methods, the minimum value of the target localization error CRLB can be derived theoretically when the receiving station is arranged at an identical angle around the target [20,21]. Ref. [22] uses polar coordinates to decouple the influence of distance and angle, and then developed the optimal deployment scheme for TOA, TDOA, and AOA sensors in remote localization scenarios based on the minimal value of CRLB. TDOA and TOA both have the same optimal deployment form, which is a ring array with the same number of nodes on each ring. In [23], the AOA-based two-dimensional station deployment strategy is extended to a three-dimensional scenario, and it is proposed that when N stations ($N \geq 4$) are spatially equidistant from the target, the optimal geometry between the sensor and the target is a uniform distribution of N stations on a unit sphere with the target at the center of the circle. For the CRLB minimization problem in the TDOA localization scenario, [24,25] investigated the optimization of ground station deployment for TDOA localization utilizing the GA algorithm and particle swarm algorithm, with CRLB minimization as the objective function, and produced superior results. In [26], TOA-based sound source localization was investigated, and the adaptive GA algorithm was employed to determine the optimal sensor placement scheme based on the probability distributions of target occurrence in the area.

Against this background, we propose a hybrid source localization technique that incorporates TOA and TDOA measurement information to boost the localization precision of moving targets to the maximum extent possible. To the best of our knowledge, most of the research has centered on individual TOA or TDOA localization algorithms, performance analysis, and placement optimization, but the hybrid source localization technique has received less attention. First, the fundamental architecture of the hybrid source localization system is developed and investigated by combining TOA and TDOA measurement information. Secondly, an iterative localization algorithm based on the least squares criterion is proposed, and the performance of localization error and CRLB is quantified through theoretical analysis and experimental simulations. Finally, the average CRLB value of target line trajectory localization error is used as the performance estimation objective function, and a GA algorithm is introduced to search for the optimal station placement scheme for TOA and TDOA hybrid source localization, the general principles of optimal station placement are given, and the localization performance is simulated and validated under various scenario configurations.

The rest of this paper is structured as follows. Section 2 analyzes the TOA/TDOA system model, while the structure of the proposed TOA/TDOA algorithm and simulation results are discussed in further detail. In Section 3, we derive the positioning error and CRLB and study their properties. Section 4 presents the simulation results of TOA, TDOA, and TOA/TDOA positioning accuracy to demonstrate the proposed system's placement optimization. Finally, Section 5 provides conclusions.

2. Hybrid Source Localization Based on TOA and TDOA

2.1. Hybrid Source Localization Algorithm Model

As shown in Figure 1, we consider three-station TOA and four-station TDOA localization systems in three-dimensional space, where the TOA system is composed of three observation stations denoted as S_4, S_5, and S_6, and the TDOA system is composed of four observation stations denoted as D_0, D_1, D_2, and D_3. The position coordinates of each station are denoted as $D_i = [x_i\ y_i\ z_i]^T$, $i = 0 \sim 3$, $S_i = [x_i\ y_i\ z_i]^T$, $i = 4 \sim 6$, and the coordinate of the signal source is $T = [x\ y\ z]^T$.

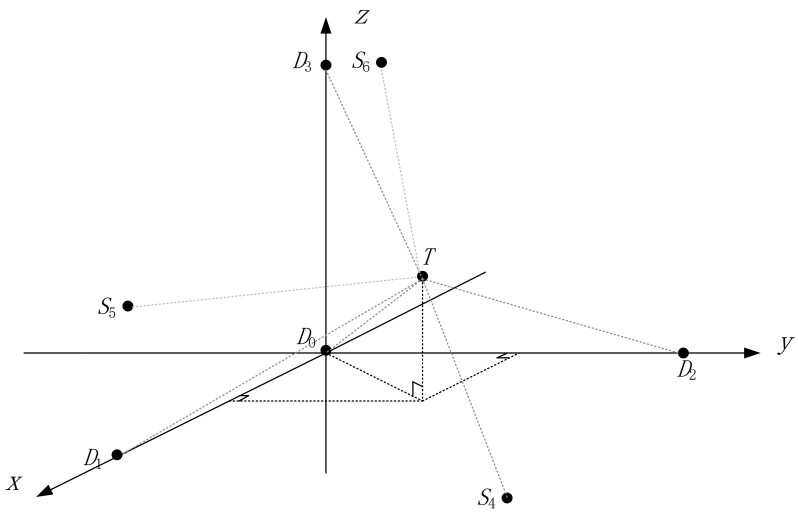

Figure 1. Systematic scenario of hybrid source localization technique.

The distance and difference in distance between each station in the TDOA positioning system and signal source T are given as follows

$$r_i = \sqrt{(x - x_i)^2 + (y - y_i)^2 + (z - z_i)^2},\ i = 0 \sim 3 \quad (1)$$

$$r_{TDOA,\,i} = r_i - r_0 = \sqrt{(x - x_i)^2 + (y - y_i)^2 + (z - z_i)^2} - \sqrt{(x - x_0)^2 + (y - y_0)^2 + (z - z_0)^2},\ i = 1 \sim 3 \quad (2)$$

Similarly, the distance between each station in the TOA positioning system and signal source T are stated as follows:

$$r_{TOA,\,i} = \sqrt{(x - x_i)^2 + (y - y_i)^2 + (z - z_i)^2},\ i = 4 \sim 6 \quad (3)$$

Combining Equations (2) and (3) yields the function matrix $\boldsymbol{f}(\boldsymbol{x})$ as

$$\boldsymbol{f}(\boldsymbol{x}) = \begin{pmatrix} \sqrt{(x-x_4)^2+(y-y_4)^2+(z-z_4)^2} \\ \sqrt{(x-x_5)^2+(y-y_5)^2+(z-z_5)^2} \\ \sqrt{(x-x_6)^2+(y-y_6)^2+(z-z_6)^2} \\ \sqrt{(x-x_1)^2+(y-y_1)^2+(z-z_1)^2} \\ \sqrt{(x-x_2)^2+(y-y_2)^2+(z-z_2)^2} \\ \sqrt{(x-x_3)^2+(y-y_3)^2+(z-z_3)^2} \end{pmatrix} - \begin{pmatrix} 0 \\ 0 \\ 0 \\ \sqrt{(x-x_0)^2+(y-y_0)^2+(z-z_0)^2} \\ \sqrt{(x-x_0)^2+(y-y_0)^2+(z-z_0)^2} \\ \sqrt{(x-x_0)^2+(y-y_0)^2+(z-z_0)^2} \end{pmatrix} \tag{4}$$

The measured values of TOA and TDOA are represented as $\widetilde{r}_{TOA}$ and $\widetilde{r}_{TDOA}$, respectively. The complete measurement result is given as $\widetilde{\boldsymbol{r}} = [\widetilde{r}_{TOA,4}\ \widetilde{r}_{TOA,5}\ \widetilde{r}_{TOA,6}\ \widetilde{r}_{TDOA,1}\ \widetilde{r}_{TDOA,2}\ \widetilde{r}_{TDOA,3}]^T$. The TOA and TDOA measurement positioning models can then be expressed as

$$\widetilde{\boldsymbol{r}} = \boldsymbol{f}(\boldsymbol{x}) + \boldsymbol{n} \tag{5}$$

where $\boldsymbol{n}$ is the measured noise vector and satisfies the random probability distribution.

Solving Equation (5) yields the position vector $\boldsymbol{x}$. Typically, there are two types of solution algorithms: linear and nonlinear. Nonlinear approaches are more computationally intensive but more accurate, and often use least squares or maximum likelihood estimators to estimate the position vector $\boldsymbol{x}$. There are two types of least squares methods, weighted and unweighted, when the measurement noise $\boldsymbol{n}$ conforms to the zero-mean Gaussian distribution, weighted least squares are identical to the maximum likelihood estimation. Weighted least squares employ the inverse matrix of the measurement noise's covariance matrix to weigh the square of the error. Although this algorithm's accuracy performance has increased, it is less stable than least squares and is prone to large errors.

The nonlinear least squares estimator can be used to continuously approximate the position vector $\boldsymbol{x}$ through iterative operations, and the regular iterative algorithms are the Newton–Raphson method, the Gauss–Newton method, and the steepest descent method [13], among which the steepest descent method is highly stable but slow to converge, and the Newton–Raphson method and Gauss–Newton method are fast to converge, but have poor stability, and require matrix inversion with a large amount of calculation. Levenberg–Marquardt algorithm combines the advantages of the Gauss–Newton method and steepest descent method, and by adding the judgment condition of first-order approximation and weighting the two algorithms, it can improve the stability of the algorithm and accelerate the convergence speed of the algorithm at the same time. The DOG-LEG algorithm based on the steepest descent method, which adjusts the step according to the gradient change of $\boldsymbol{f}(\boldsymbol{x})$, can improve the convergence speed.

Let $\boldsymbol{F}(\boldsymbol{x}) = \widetilde{\boldsymbol{r}} - \boldsymbol{f}(\boldsymbol{x})$, the nonlinear least squares estimation can be used to find the $\hat{\boldsymbol{x}}$, that minimizes the sum-of-squares function of the nonlinear error function $J(\boldsymbol{x})$

$$J(\boldsymbol{x}) = \| \boldsymbol{F}(\boldsymbol{x})^2 \| = \| \widetilde{\boldsymbol{r}} - \boldsymbol{f}(\boldsymbol{x})^2 \| = (\widetilde{\boldsymbol{r}} - \boldsymbol{f}(\boldsymbol{x}))^T(\widetilde{\boldsymbol{r}} - \boldsymbol{f}(\boldsymbol{x})) \tag{6}$$

$$\hat{\boldsymbol{x}} = \arg\min_{\boldsymbol{x}} J(\boldsymbol{x}) \tag{7}$$

The Gauss-Newton method is employed to obtain the iterative equation for the estimation of $\hat{\boldsymbol{x}}$ as

$$\hat{\boldsymbol{x}}^{k+1} = \hat{\boldsymbol{x}}^k + (G^T\left(\hat{\boldsymbol{x}}^k\right)G\left(\hat{\boldsymbol{x}}^k\right))^{-1}G^T\left(\hat{\boldsymbol{x}}^k\right)\left(\widetilde{\boldsymbol{r}} - \boldsymbol{f}\left(\hat{\boldsymbol{x}}^k\right)\right) \tag{8}$$

$\boldsymbol{G}(\boldsymbol{x}) = \nabla^T\left(\boldsymbol{f}^T(\boldsymbol{x})\right)$, substituting $\boldsymbol{f}(\boldsymbol{x})$ into the equation and simplifying it gives

$$\boldsymbol{G}(\boldsymbol{x}) = \begin{pmatrix} \frac{x-x_4}{r_4} & \frac{x-x_5}{r_5} & \frac{x-x_6}{r_6} & \frac{x-x_1}{r_1} - \frac{x-x_0}{r_0} & \frac{x-x_2}{r_2} - \frac{x-x_0}{r_0} & \frac{x-x_3}{r_3} - \frac{x-x_0}{r_0} \\ \frac{y-y_4}{r_4} & \frac{y-y_5}{r_5} & \frac{y-y_6}{r_6} & \frac{y-y_1}{r_1} - \frac{y-y_0}{r_0} & \frac{y-y_2}{r_2} - \frac{y-y_0}{r_0} & \frac{y-y_3}{r_3} - \frac{y-y_0}{r_0} \\ \frac{z-z_4}{r_4} & \frac{z-z_5}{r_5} & \frac{z-z_6}{r_6} & \frac{z-z_1}{r_1} - \frac{z-z_0}{r_0} & \frac{z-z_2}{r_2} - \frac{z-z_0}{r_0} & \frac{z-z_3}{r_3} - \frac{z-z_0}{r_0} \end{pmatrix}^T \tag{9}$$

2.2. Analysis of Positioning Accuracy Analysis

2.2.1. Least Squares Localization Error Analysis

The precision of positioning is determined by two factors: the measurement error and the geometric factor of the positioning error, which are usually coupled together. The geometric factor of the measurement error and the positioning error are usually mixed together, but can be considered separately and independently only when the measurement noise of each signal source is independent and has the same variance. Independent consideration of the geometric factors of measurement error and positioning error facilitates the separate evaluation of the station placement scheme, and the geometric factor of positioning error is usually expressed as GDOP, which can also be expressed as HDOP (horizontal) or DOP in the direction of the other axis. The measurement error generally includes the station location positioning error of each station and the measurement error of TOA and TDOA, which are considered to be independent of each other, and the measurement error of TOA and TDOA includes the signal propagation error, synchronization error between measurement stations, a random error caused by receiver noise, Doppler effect error, etc.

Considering the error terms of TDOA, it is obtained from (2) that

$$\begin{aligned} d(r_{TDOA,\,i}) = dr_i - dr_0 = d\Big(&\sqrt{(x-x_i)^2+(y-y_i)^2+(z-z_i)^2} \\ &-\sqrt{(x-x_0)^2+(y-y_0)^2+(z-z_0)^2}\Big) \\ = (g_{ix}-g_{0x})dx + &\left(g_{iy}-g_{0y}\right)dy + \left(g_{iy}-g_{0y}\right)dz - h_i + h_0,\ i = 1,2,3 \end{aligned} \tag{10}$$

where

$$g_{ix} = \frac{x-x_i}{\sqrt{(x-x_i)^2+(y-y_i)^2+(z-z_i)^2}} \tag{11}$$

$$g_{iy} = \frac{y-y_i}{\sqrt{(x-x_i)^2+(y-y_i)^2+(z-z_i)^2}} \tag{12}$$

$$g_{iz} = \frac{z-z_i}{\sqrt{(x-x_i)^2+(y-y_i)^2+(z-z_i)^2}} \tag{13}$$

$$h_i = g_{ix}dx_i + g_{iy}dy_i + g_{iz}dz_i \tag{14}$$

$d(r_{TDOA\ i})$ represents the measurement error of distance difference, dx_i,dy_i, dz_i are the measurement errors of the station positions in the three-coordinate axis. dx,dy,dz are signal source T positioning errors. Combine the three equations in (10), and let

$$\boldsymbol{G}_{TDOA} = \begin{pmatrix} g_{1x}-g_{0x} & g_{1y}-g_{0y} & g_{1z}-g_{0z} \\ g_{2x}-g_{0x} & g_{2y}-g_{0y} & g_{2z}-g_{0z} \\ g_{3x}-g_{0x} & g_{3y}-g_{0y} & g_{3z}-g_{0z} \end{pmatrix}$$

$$d\boldsymbol{x}_{s\ \mathrm{TDOA}} = \begin{pmatrix} h_1-h_0 \\ h_2-h_0 \\ h_3-h_0 \end{pmatrix},\ d\boldsymbol{x} = \begin{pmatrix} dx \\ dy \\ dz \end{pmatrix}$$

$$d\boldsymbol{r}_{TDOA} = \begin{pmatrix} d(r_{TDOA,\ 1}) \\ d(r_{TDOA,2}) \\ d(r_{TDOA,3}) \end{pmatrix} = \begin{pmatrix} dr_1-dr_0 \\ dr_2-dr_0 \\ dr_3-dr_0 \end{pmatrix}$$

Then we have

$$\boldsymbol{G}_{TDOA}d\boldsymbol{x} = d\boldsymbol{r}_{TDOA} + d\boldsymbol{x}_{s\ \mathrm{TDOA}} \tag{15}$$

Considering the error terms of TOA, from (3) we can obtain

$$dr_i = d\left(\sqrt{(x-x_i)^2+(y-y_i)^2+(z-z_i)^2}\right) = g_{ix}dx + g_{iy}dy + g_{iz}dz - h_i,\ i = 4,5,6 \tag{16}$$

Presents the simultaneous equations from 4 to 6 of (16), and let

$$\boldsymbol{G}_{TOA} = \begin{pmatrix} g_{4x} & g_{4y} & g_{4z} \\ g_{5x} & g_{5y} & g_{5z} \\ g_{6x} & g_{6y} & g_{6z} \end{pmatrix},\ d\boldsymbol{x}_{s\ \mathrm{TOA}} = \begin{pmatrix} h_4 \\ h_5 \\ h_6 \end{pmatrix},\ d\boldsymbol{r}_{TOA} = \begin{pmatrix} dr_4 \\ dr_5 \\ dr_6 \end{pmatrix}$$

Then we have

$$\boldsymbol{G}_{TOA} d\boldsymbol{x} = d\boldsymbol{r}_{TOA} + d\boldsymbol{x}_{s\ \mathrm{TOA}} \tag{17}$$

Combining Equations (15) and (17) to obtain

$$\boldsymbol{G} d\boldsymbol{x} = d\boldsymbol{r} + d\boldsymbol{x}_s \tag{18}$$

where

$$\boldsymbol{G} = [\boldsymbol{G}_{TOA}^T\ \boldsymbol{G}_{TDOA}^T]^T,\ d\boldsymbol{r} = [d\boldsymbol{r}_{TOA}^T\ d\boldsymbol{r}_{TDOA}^T]^T,\ d\boldsymbol{x}_s = [d\boldsymbol{x}_{s\ TOA}^T\ d\boldsymbol{x}_{s\ TDOA}^T]^T \tag{19}$$

The error value of Least square estimation is denoted as

$$d\boldsymbol{x} = (\boldsymbol{G}^T\boldsymbol{G})^{-1}\boldsymbol{G}^T(d\boldsymbol{r} + d\boldsymbol{x}_s) \tag{20}$$

The covariance matrix of positioning error is

$$\left[d\boldsymbol{x}d\boldsymbol{x}^T\right] = (\boldsymbol{G}^T\boldsymbol{G})^{-1}\boldsymbol{G}^T E\left[(d\boldsymbol{r} + d\boldsymbol{x}_s)\left(d\boldsymbol{r} + d\boldsymbol{x}_s\right)^T\right]\boldsymbol{G}(\boldsymbol{G}^T\boldsymbol{G})^{-1} \tag{21}$$

Given that the station location positioning errors dx_i,dy_i,dz_i are independent, as are the measurement errors dr_i, the station location positioning errors and measurement errors are independent as well, and the mean values are all zero. The variance of station location positioning errors can be expressed as $E[(dx_i)^2] = E[(dy_i)^2] = E[(dz_i)^2] = \sigma_s^2$, and the measurement errors can be denoted as $E[(dr)^2] = \sigma_m^2$.

$$E[(d\boldsymbol{r} + d\boldsymbol{x}_s)\left(d\boldsymbol{r} + d\boldsymbol{x}_s\right)^T] = E[d\boldsymbol{r}d\boldsymbol{r}^T] + E\left[d\boldsymbol{x}_s d\boldsymbol{x}_s{}^T\right] \tag{22}$$

$$E\left[d\boldsymbol{r}d\boldsymbol{r}^T\right] = E\left(\begin{pmatrix} d\boldsymbol{r}_{TOA} \\ d\boldsymbol{r}_{TDOA} \end{pmatrix}\begin{pmatrix} d\boldsymbol{r}_{TOA} \\ d\boldsymbol{r}_{TDOA} \end{pmatrix}^T\right) = blkdiag\left(diag\left(\left[\sigma_m^2\ \sigma_m^2\ \sigma_m^2\right]\right), diag\left(\left[\sigma_m^2\ \sigma_m^2\ \sigma_m^2\right]\right) + \sigma_m^2 \bullet ones(3,3)\right) \tag{23}$$

$$E\left[d\boldsymbol{x}_s d\boldsymbol{x}_s{}^T\right] = E\left(\begin{pmatrix} d\boldsymbol{x}_{s\ \mathrm{TOA}} \\ d\boldsymbol{x}_{s\ \mathrm{TDOA}} \end{pmatrix}\begin{pmatrix} d\boldsymbol{x}_{s\ \mathrm{TOA}} \\ d\boldsymbol{x}_{s\ \mathrm{TDOA}} \end{pmatrix}^T\right) = blkdiag\left(diag\left(\left[\sigma_s^2\ \sigma_s^2\ \sigma_s^2\right]\right), diag\left(\left[\sigma_s^2\ \sigma_s^2\ \sigma_s^2\right]\right) + \sigma_s^2 \bullet ones(3,3)\right) \tag{24}$$

where *blkdiag*{.}: Block diagonal matrix operator in MATLAB, *blkdiag*(*A*,*B*) represents a matrix with matrices *A* and *B* as diagonal blocks; *diag*{.}: Diagonal matrix operator in MATLAB, *diag*(*a*) represents a matrix with the elements of vector *a* as diagonal elements; *ones*{.}: define a matrix with all elements equal to 1 in MATLAB, *ones*{*a*,*b*} represents an all 1 matrix with the size of a row and b column.

$E\left[d\boldsymbol{r}d\boldsymbol{r}^T\right]$ and $E\left[d\boldsymbol{x}_s d\boldsymbol{x}_s{}^T\right]$ have the same form, and the variance $E\left[(d\boldsymbol{r} + d\boldsymbol{x}_s)\left(d\boldsymbol{r} + d\boldsymbol{x}_s\right)^T\right]$ can be obtained after adding the two terms. The station location error and measurement error can be combined as the same noise source, so the two items can be considered equivalently; that is, the station location positioning error and the measurement error variance are summed as the total error, and let $\sigma^2 = \sigma_m^2 + \sigma_s^2$, then the positioning estimation error covariance matrix $\boldsymbol{C}$ with least squares estimation can be denoted as

$$\boldsymbol{C} = E\left[(d\boldsymbol{r} + d\boldsymbol{x}_s)\left(d\boldsymbol{r} + d\boldsymbol{x}_s\right)^T\right] = \begin{pmatrix} \sigma^2 & 0 & 0 & 0 & 0 & 0 \\ 0 & \sigma^2 & 0 & 0 & 0 & 0 \\ 0 & 0 & \sigma^2 & 0 & 0 & 0 \\ 0 & 0 & 0 & 2\sigma^2 & \sigma^2 & \sigma^2 \\ 0 & 0 & 0 & \sigma^2 & 2\sigma^2 & \sigma^2 \\ 0 & 0 & 0 & \sigma^2 & \sigma^2 & 2\sigma^2 \end{pmatrix} \tag{25}$$

The covariance matrix of positioning error $\boldsymbol{\sigma}^2$ based on least square estimation is denoted as

$$\boldsymbol{\sigma}^2 = E\left[d\boldsymbol{x}d\boldsymbol{x}^T\right] = \left(\boldsymbol{G}^T\boldsymbol{G}\right)^{-1}\boldsymbol{G}^T\boldsymbol{C}\boldsymbol{G}\left(\boldsymbol{G}^T\boldsymbol{G}\right)^{-1} \tag{26}$$

The positioning error can be denoted as $Tr\left(\boldsymbol{\sigma}^2\right)$.

2.2.2. Cramer Rao Bound

Cramer Rao Low Bound (CRLB) gives a lower bound on the variance of the unbiased estimator and can serve as an essential comparison indicator for the performance of the estimation algorithm. As can be seen from the previous analysis, the measurement error $\boldsymbol{n}$ in Equation (5) can be regarded as the sum of station location positioning error and measurement error, which generally satisfies the zero mean Gaussian distribution, so the probability density function of TOA and TDOA measurements can be expressed as

$$\boldsymbol{p}(\widetilde{\boldsymbol{r}}) = \frac{\mathbf{1}}{(\mathbf{2}\boldsymbol{\pi})^{\frac{L}{2}}|\boldsymbol{C}|^{\frac{1}{2}}}\boldsymbol{exp}\left(-\frac{\mathbf{1}}{\mathbf{2}}(\widetilde{\boldsymbol{r}} - \boldsymbol{f}(\boldsymbol{x}))\boldsymbol{C}^{-\mathbf{1}}(\widetilde{\boldsymbol{r}} - \boldsymbol{f}(\boldsymbol{x}))\right) \tag{27}$$

CRLB is equal to the trace of the inverse matrix $\boldsymbol{I}(\boldsymbol{x})$ of the Fisher information matrix (FIM) [27]

$$\begin{aligned} CRLB &= [\boldsymbol{I}(\boldsymbol{x})]^{-1} = E[(\partial \ln(p(\widetilde{\boldsymbol{r}}))/\partial \boldsymbol{x}^T)(\partial \ln(p(\widetilde{\boldsymbol{r}}))/\partial \boldsymbol{x}^T)^T]^{-1} \\ &= \left(\left[\frac{\partial f(x)}{\partial x}\right]\boldsymbol{C}^{-1}\left[\frac{\partial f(x)}{\partial x}\right]^T\right)^{-1} \end{aligned} \tag{28}$$

where $\partial \boldsymbol{f}(\boldsymbol{x})/\partial \boldsymbol{x}$ is the transpose matrix of $\boldsymbol{G}$ in Equation (19), and then we can obtain the positioning error

$$\text{positioningerror} = Tr[CRLB] \tag{29}$$

3. Genetic Algorithm-Based Optimization of the Station Placement Scheme

The objective of the station placement scheme optimization is to optimize the deployment of stations according to the target trajectory to be measured so that the total positioning error is minimized [28], and the CRLB is used as the objective function of the optimized placement due to the consistency of the CRLB and LS positioning errors. The positioning error function can be expressed as

$$\text{positioningerror} = \frac{1}{V}\int_{x_a}^{x_b}\int_{y_a(x)}^{y_b(x)}\int_{z_a(x,y)}^{z_b(x,y)}\sqrt{Tr(CRLB)}dxdydz \tag{30}$$

where x_a, x_b, $y_a(x)$, $y_b(x)$, $z_a(x,y)$, $z_b(x,y)$ are corresponding to the upper and lower integral limits of variable x, y, z. V is the volume of the entire integral space.

Since the function in Equation (30) is nonlinear and nonconvex, we use a Genetic Algorithm (GA) to solve for the optimal station deployment scheme. A GA algorithm is a stochastic search algorithm that draws on natural selection and natural genetic mechanisms in biology and is very suitable for dealing with complex, nonconvex, and nonlinear optimization problems that are difficult to solve by traditional search algorithms. Unlike traditional search algorithms, GA algorithms start from a randomly generated initial solution and iterate step by step through a series of selection, crossover, and mutation operations to generate a new solution. A certain number of sound individuals are selected from the previous generation according to their fitness, and the next generation population is formed by crossover and mutation. After several generations of evolution, the algorithm converges on the best chromosome, which is the optimal or suboptimal solution to the problem. Genetic algorithm has strong global search ability, but weak local search ability, and usually can only get the suboptimal solution of the problem, but not the optimal solution. Classical nonlinear programming algorithms mostly use the gradient descent method to solve the problem, which has a stronger local search ability but a weaker global search ability. Therefore, this paper combines the advantages of both algorithms, using a Genetic Algorithm for global search on the one hand and a nonlinear programming algorithm for local search on the other hand, so that the global optimal solution of the station placement scheme can be obtained.

In practical applications, TOA and TDOA measurement stations are generally deployed on the ground, and the range of station placement is limited to a certain range due to the influence of radio link receiving distance. Therefore, it is necessary to put additional constraints on the station range in the GA algorithm, i.e., the station location is constrained to be within the square formed by four points in the XOY plane (-8×10^3, -5×10^3), (-5×10^3, 5×10^3), (5×10^3, -5×10^3), and (5×10^3, 5×10^3). The target trajectory is to be located in a line from point (5×10^2, 5×10^2) to point (5×10^3, 5×10^3) in the YOZ plane and the positioning error is calculated according to Equation (30) to find the optimal station location estimation vector $\hat{\theta}$ to minimize the positioning error.

$$\hat{\theta} = \underset{\theta}{\operatorname{argmin}}\left(\frac{1}{V}\int_{x_a}^{x_b}\int_{y_a(x)}^{y_b(x)}\int_{z_a(x,y)}^{z_b(x,y)}\sqrt{Tr(CRLB)}dxdydz\right) \tag{31}$$

where $\theta = [x_1\ y_1\ x_2\ y_2 \cdot \cdot \cdot x_N\ y_N]$, N is the number of ground TOA and TDOA stations.

4. Simulation Experiment and Performance Analysis

4.1. Simulation Results of Hybrid Source Localization Algorithms

According to Equations (8) and (9), TOA, TDOA, and TOA and TDOA hybrid source localization are simulated, and the Gauss–Newton method is adopted for the localization iterative algorithm. The simulation results are shown in Figure 2, with the horizontal coordinate as the measurement variance and the vertical coordinate as the positioning error. TOA stations' coordinates are $S_4(1 \times 10^4\ 0\ 0)$, $S_5(0\ 1 \times 10^4\ 0)$, and $S_6(0\ 0\ 1 \times 10^4)$, the TDOA stations' coordinates are $D0(0\ 0\ 0)$, $D1(1 \times 10^4\ 0\ 0)$, $D_2(0\ 1 \times 10^4\ 0)$, and $D_3(0\ 0\ 1 \times 10^4)$. Target's coordinate is $T(5 \times 10^3\ 5 \times 10^3\ 5 \times 10^3)$. The measurement variance in Figure 2 is the noise variance in Equation (5), which satisfies the zero mean Gaussian distribution. Figure 2a shows the error curves of 3-TOA positioning stations (asterisks), 4-TDOA positioning stations (triangle), 1-TOA and 4-TDOA hybrid positioning stations (circle). Figure 2b,c also corresponds to the error curves of also 3-TOA stations and 4-TDOA positioning errors, while the hybrid positioning error curves are corresponding to 2-TOA/4-TDOA hybrid source localization, and 3-TOA/4-TDOA hybrid source localization. Figure 2c also shows a 3-TOA Cramer Rao Low Boundary (CRLB) curve. Figure 2a–c also show a 3-TOA CRLB Boundary curve. Figure 2d illustrates the spatial distribution of each station.

It can be seen from Figure 2 that the accuracy of 3-station TOA positioning and 4-station TDOA positioning is essentially the same, which is consistent with the Cramer Rao boundary of 3-station TOA positioning, while the accuracy of hybrid source localization is higher than the individual positioning accuracy of the two methods alone, and the error of the TOA and TDOA hybrid source localization gradually decreases with the gradual increase in TOA stations, i.e., an increase in the amount of TOA stations and TDOA stations can improve the positioning precision.

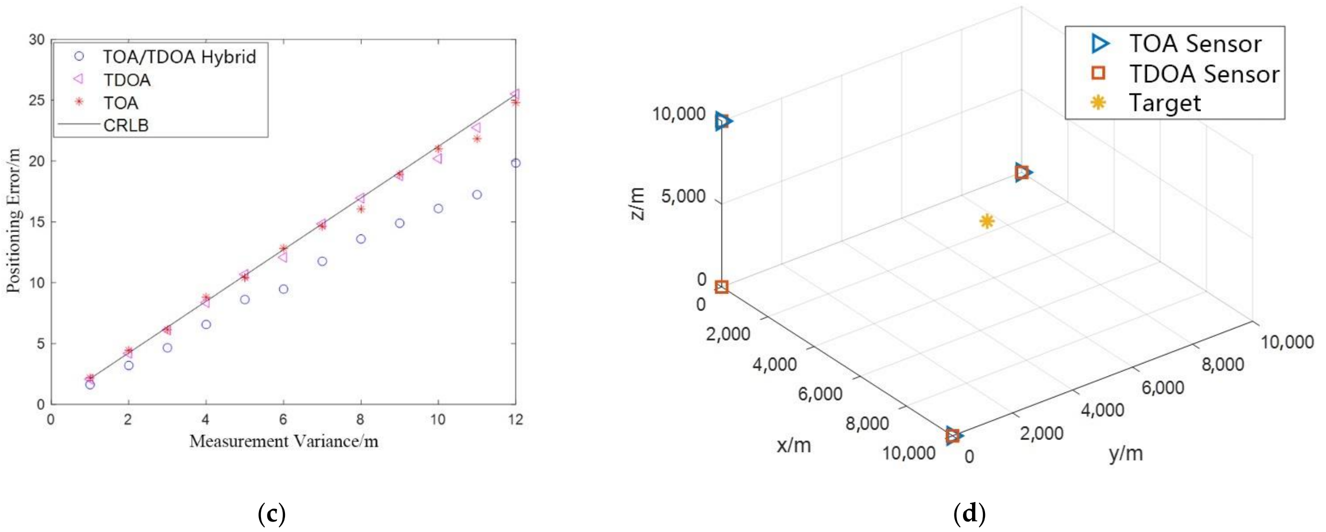

Figure 2. TOA/TDOA hybrid positioning simulation curve based on Gauss–Newton method: (**a**) Simulation results for 1-TOA sensor and 4-TDOA sensors; (**b**) Simulation results for 2-TOA sensor and 4-TDOA sensors; (**c**) Simulation results for 3-TOA sensor and 4-TDOA sensors; (**d**) Placement scheme for 3-TOA sensor and 4-TDOA sensors.

4.2. Simulation Analysis of Positioning Accuracy of Typical Placement Topology Structure

Based on the previous analysis of solution accuracy on TOA, TDOA, and TOA/TDOA hybrid positioning, we give the simulation results and comparative analysis on positioning error spatial distribution of CRLB and least square algorithms with three kinds of solution accuracy. During the simulation, we assume the variance of measurement and position $\sigma^2 = 1$; therefore, the positioning error is equivalent to the value of GDOP. The spatial distribution of GDOP is calculated according to the line trajectory, and three-dimensional spatial station placement is adopted, as shown in Figure 3. We consider seven stations when calculating the TOA/TDOA hybrid positioning errors, that is, TOA stations are marked as $S_4(1 \times 10^4\ 0\ 0)$, $S_5(0\ 1 \times 10^4\ 0)$, and $S_6(0\ 0\ 1 \times 10^4)$, the TDOA stations are marked as $D_0(0\ 0\ 0)$, $D_1(1 \times 10^4\ 0\ 0)$, $D_2(0\ 1 \times 10^4\ 0)$, and $D_3(0\ 0\ 1 \times 10^4)$.

For the three-dimensional spatial station deployment, we carried out the GDOP distribution calculation for the line trajectory parallel to the Z-axis and varying in height from 1000 m to 10,000 m, as shown in Figure 4. It can be seen from the figure that the difference between the LS positioning solution error and the theoretical value of CRLB is basically the same; only the LS error is slightly larger than CRLB when the hybrid source localization solution is applied, and the LS error is also marginally higher than CRLB when the stationing placement scheme is altered, but in general, the LS positioning calculation error is close to CRLB, and it is robust and does not require a priori knowledge, such as noise distribution, to obtain.

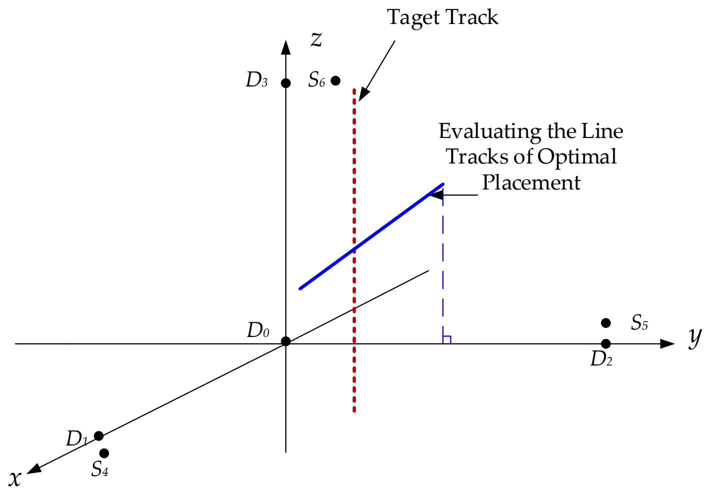

Figure 3. Schematic Diagram of Receiving Station Placement and Target Line Trajectory for TOA/TDOA hybrid source localization system.

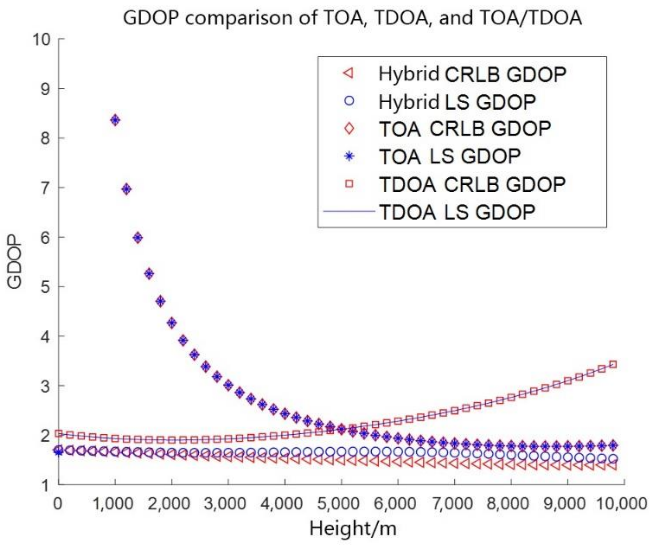

Figure 4. GDOP curves of TOA, TDOA, and TOA/TDOA hybrid positioning of line trajectory.

The GDOP of TDOA is more uniformly distributed with little performance deterioration, while the GDOP of TOA suddenly deteriorates sharply at a certain position in the low altitude, and the deterioration region is caused by the inverse of the sick matrix due to the rank of the matrix **G** dropping to 2 due to the coplanarity of S_4, S_5, and S_6. The GDOP accuracy of the hybrid source localization is better than the separate localization accuracy of TOA or TDOA alone, which is consistent with the results of the previous localization solution in Figure 2.

4.3. Simulation Results of Placement Optimization Based on Genetic Algorithm

We set the main parameters of the GA algorithm for the scenario in this paper: the population size is taken as 200, the selection parameter is chosen as 0.05 multiplied by the population size, the crossover probability is set as 0.8, and the variogram function parameters Scale and Shrink are both taken as 1 to ensure that global optimization is achieved within the range of values taken. The number of iterations is adjusted according to the number of stations to be deployed, which is obtained by multiplying the number of stations by 600. The accuracy of the variables is chosen as 1×10^{-3}, and the accuracy of the objective function calculation is chosen as 1×10^{-6}. The target's line trajectory varies from point (5×10^2, 5×10^2) to point (5×10^3, 5×10^3) in the YOZ plane, as shown in Figure 3.

Figure 5 shows the simulation results of the optimal GA algorithm-based station deployment scheme under different numbers of TOA and TDOA stations, where the asterisks in Figure 5a give the simulation results of optimal station placement for five TDOA stations and the asterisks in Figure 5b give the simulated results of optimal station placement for seven TDOA stations. From the figure, it can be seen that when there are only TDOA stations, the optimal station placement is generally symmetric around the target line trajectory, and the station locations are mainly spread out at the four corners of the boundary and below the target trajectory line. When there is a combination of TOA and TDOA stations, the optimization algorithm gives the station placement scheme as shown in Figure 5c,d, where the TDOA stations are mainly located at the four corners of the boundary and the TOA stations are mainly located below the target line trajectory.

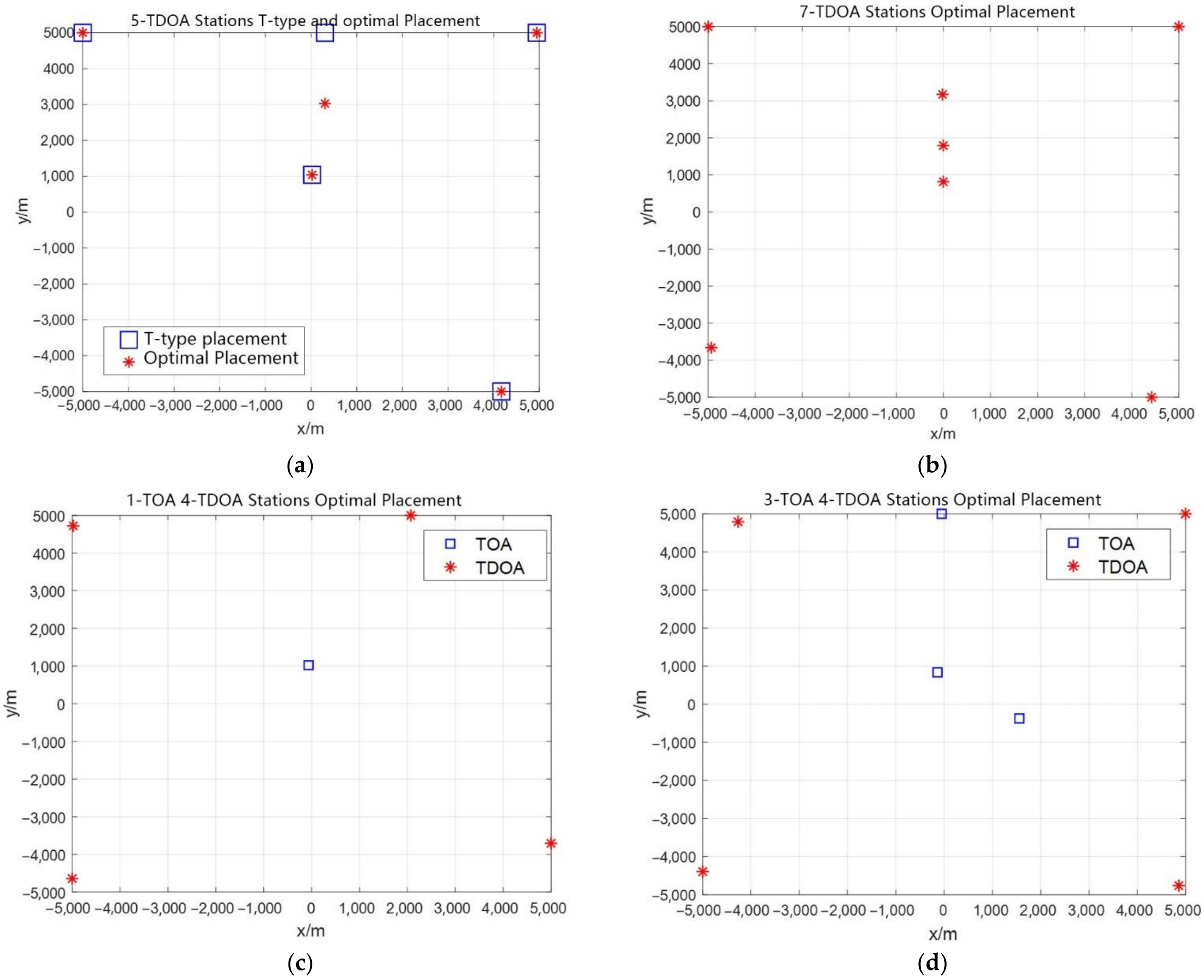

Figure 5. Optimal station placement results based on GA algorithm: (**a**) 5-TDOA stations T-type placement and optimized layout structure; (**b**) Optimized layout structure for 7-TDOA stations; (**c**) Optimized layout structure simulation for 1-TOA and 4-TDOA stations; (**d**) Optimized layout structure simulation for 3-TOA and 4-TDOA stations.

Based on the optimization results of each of the above placement schemes, we obtained the positioning accuracy or GDOP curve of the target line trajectory from point (5×10^2, 5×10^2) to point (5×10^3, 5×10^3) in the YOZ plane by simulation, as shown in Figure 6. The line trajectory positioning accuracy curves of the T-shaped placement scheme are also added in Figure 6, and the T-shaped placement scheme is shown in Figure 5a. It can be seen from the figure that when there are five TDOA stations, except for the positioning accuracy of the optimal deployment scheme and the T-type placement scheme at the height of 500 m–900 m, which is essentially the same, the positioning accuracy of the optimal deployment scheme for other points of the line trajectory is better than that of the T-type deployment station, which indicates that the optimization effect of the GA algorithm on the placement scheme is apparent. Meanwhile, the positioning accuracy improves with the increase in the number of stations, for example, the positioning accuracy of 7 TDOA stations is better than that of 5 TDOA stations, and the positioning accuracy of 3 TOA stations plus 4 TDOA stations is better than that of 1 TOA station plus 4 TDOA stations. In addition, the improvement effect of TOA station on positioning accuracy is better than that of TDOA station, and the performance of hybrid source localization of TOA plus TDOA is better than that of pure TDOA positioning, for instance, the positioning accuracy of 1 TOA station plus 4 TDOA stations is better than that of 5 TDOA stations or 7 TDOA stations, and the hybrid source localization accuracy of TOA and TDOA stations does not deteriorate much with the increase in height, while the pure TDOA station positioning accuracy deteriorates more significantly with the increase in altitude.

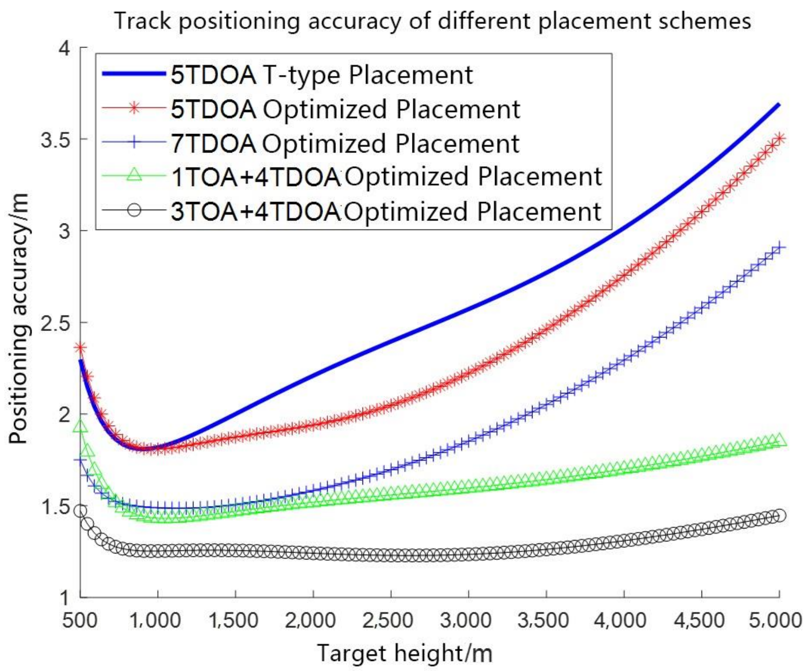

Figure 6. Target trajectory positioning accuracy of different station layout schemes.

Compared with the above-mentioned station placement schemes, the positioning accuracy of 1TOA station plus 4TDOA station can obtain higher positioning accuracy with fewer stations, and the performance of positioning accuracy is more stable, and the performance deterioration is not apparent. Figure 7 shows the contour distribution surfaces of the GDOP values in the YOZ plane for x values equal to -1×10^3, 0, and 1×10^3, respectively, for this station placement optimization scheme. From the figure, it can be seen that the GDOP distribution curves in three different YOZ profiles do not change much in both the Y-axis and Z-axis direction, which shows that the station placement optimization also has good stability in the X-axis direction. When the target trajectory to be located is in other shapes, such as when the target trajectory is a point or a region, the integral region of the objective function needs to be adjusted to obtain the corresponding optimal placement of stations.

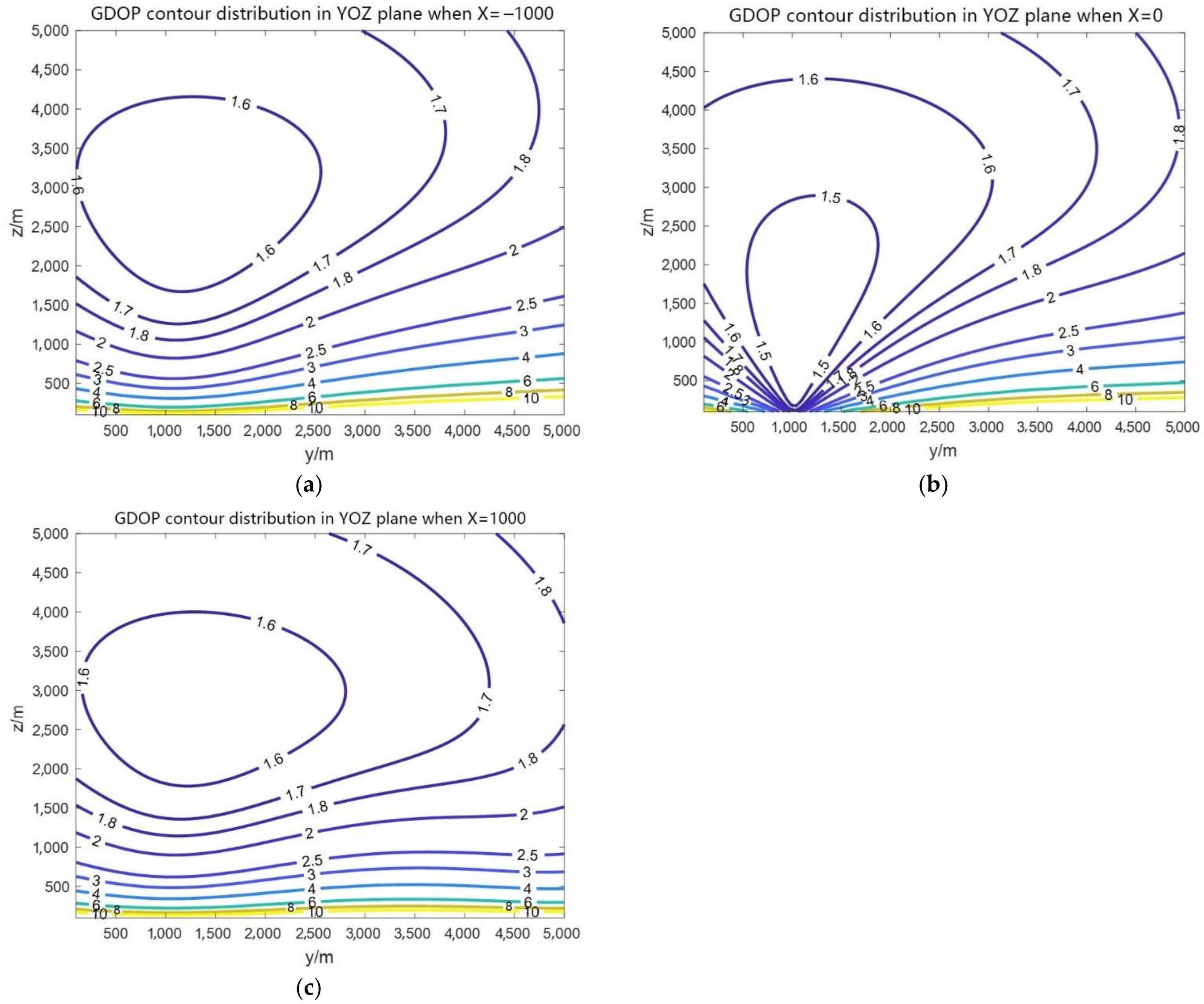

Figure 7. GDOP distribution curve of three YOZ profiles during 1TOA+4TDOA optimized station layout: (**a**) GDOP distribution of YOZ plane when $x = -1 \times 10^3$; (**b**) GDOP distribution of YOZ plane when $x = 0$; (**c**) GDOP distribution of YOZ plane when $x = 1 \times 10^3$.

5. Conclusions

In this paper, we propose a Gauss–Newton algorithm based on the least squares method to implement a hybrid TOA and TDOA positioning system for a three-dimensional spatial positioning scenario where both TOA and TDOA measurement data exist and conduct theoretical analysis and experimental simulations on the hybrid source localization system consisting of three TOA stations combined with four TDOA stations. The simulation results show that the hybrid source localization accuracy of TOA and TDOA is better than that of pure TOA or TDOA alone, and the localization performance can be significantly improved with the increase in the number of hybrid stations.

We derive the theoretical results of the least-squares estimation error and the CRLB boundary for the hybrid positioning algorithm of TOA and TDOA, and the analysis results demonstrate that the effects of the measurement error and the station location error on the positioning performance are equivalent. Simulations are performed to compare the least-squares estimation error and the CRLB boundary based on the theoretical results and the simulation results show that the least-squares estimation error and the CRLB boundary are generally consistent, which confirms the promising estimation performance of the least squares method.

For the ground station placement scenario under typical conditions, the station placement scheme is optimized by using the GA algorithm for pure TDOA positioning and TOA plus TDOA hybrid source localization with the mean value of the CRLB boundary of the target line trajectory as the objective function. The positioning errors of the optimized station placement are compared by simulation experiments, and the results demonstrate that the overall positioning accuracy of the optimized station placement scheme is better than that of the typical station placement scheme, and it is more adaptable to the trajectory form and provides better positioning performance. Finally, we summarize the general principles for the placement scheme optimization on the basis of the simulation results.

Author Contributions: Conceptualization, G.M. and J.T.; Formal analysis, G.M., Z.H. and J.T.; Investigation, G.M., M.W., Z.J. and B.S.; Methodology, G.M.; Project administration, J.T.; Supervision, X.L. and J.T.; Validation, G.M. and J.T.; Visualization, Z.H.; Writing (original draft), G.M., J.T. and M.W.; Writing (review and editing), Z.J. All authors have read and agreed to the published version of the manuscript.

Funding: This research was funded by CAEP Foundation under Grant CX20200010, National Natural Science Foundation of China: 61871084, and National Natural Science Foundation of China: 62271109.

Institutional Review Board Statement: Not applicable.

Informed Consent Statement: Not applicable.

Data Availability Statement: Not applicable.

Acknowledgments: We would like to show our deepest gratitude to Peng Fei from Rocket Force University of Engineering (Xi'an 710025, China), who has provided us with valuable guidance in every stage of this project. His efforts in providing research materials and supervising project quality, etc., enabled us to achieve a successful and efficient completion of the project.

Conflicts of Interest: The authors declare no conflict of interest.

References

1. Kanhere, O.; Rappaport, T.S. Position Location for Futuristic Cellular Communications: 5G and Beyond. *IEEE Commun. Mag.* **2021**, *59*, 70–75. [CrossRef]
2. Jürgens, S.; Koch, N.; Meinecke, M.M. Radar-based Automotive Localization using Landmarks in a Multimodal Sensor Graph-based Approach. In Proceedings of the 2020 21st International Radar Symposium (IRS), Warsaw, Poland, 5–7 October 2020; pp. 373–378.
3. Meng, T.; Zhang, Z.; Lin, Y. Joint localization algorithm of TDOA and FDOA considering the position error of underwater sensors. *IET Radar Sonar Navig.* **2022**, *16*, 1434–1445. [CrossRef]
4. Traboulsi, S. Overview of 5G-oriented Positioning Technology in Smart Cities. *Procedia Comput. Sci.* **2022**, *201*, 368–374. [CrossRef]
5. Zhao, J.; Ren, J.; Yue, H.; Lai, Z. Combined Linear Regression and Simplex Method for Signal Strength Based Indoor Position. In Proceedings of the 2008 4th International Conference on Wireless Communications, Networking and Mobile Computing, Dalian, China, 12–17 October 2008; pp. 1–4.
6. Zhao, J.; Zhang, H.; Ran, R. Distribution Localization Estimation Algorithm in Wireless Sensor Networking. In Proceedings of the 2014 IEEE 79th Vehicular Technology Conference (VTC Spring), Seoul, Republic of Korea, 18–21 May 2014; pp. 1–5.
7. Adler, A.; Wax, M. Direct Localization by Partly Calibrated Arrays: A Relaxed Maximum Likelihood Solution. In Proceedings of the 2019 27th European Signal Processing Conference (EUSIPCO), A Coruna, Spain, 2–6 September 2019; pp. 1–5.
8. Liu, G.; Liu, A.; Lian, L.; Lau, V.; Zhao, M.J. Sparse Bayesian Inference Based Direct Localization for Massive MIMO. In Proceedings of the 2019 IEEE 90th Vehicular Technology Conference (VTC2019-Fall), Honolulu, HI, USA, 22–25 September 2019; pp. 1–5.
9. Garcia, N.; Wymeersch, H.; Larsson, E.G.; Haimovich, A.M.; Coulon, M. Direct Localization for Massive MIMO. *IEEE Trans. Signal Process.* **2017**, *65*, 2475–2487. [CrossRef]
10. Zhao, J.; Liu, J.; Nie, Y.; Ni, S. Location-Assisted Beam Alignment for Train-to-Train Communication in Urban Rail Transit System. *IEEE Access* **2019**, *7*, 80133–80145. [CrossRef]
11. Drake, S.R.; Dogancay, K. Geolocation by time difference of arrival using hyperbolic asymptotes. In Proceedings of the 2004 IEEE International Conference on Acoustics, Speech, and Signal Processing, Montreal, QC, Canada, 17–21 May 2004. Ii-361.
12. Yiu-Tong, C.; Hang, H.Y.C.; Pak-chung, C. Exact and approximate maximum likelihood localization algorithms. *IEEE Trans. Veh. Technol.* **2006**, *55*, 10–16. [CrossRef]

13. Zekavat, R.; Buehrer, R.M. *Handbook of Position Location: Theory, Practice and Advances*; Wiley: Hoboken, NJ, USA, 2019.
14. Jiang, W.; Xu, C.; Pei, L.; Yu, W. Multidimensional Scaling-Based TDOA Localization Scheme Using an Auxiliary Line. *IEEE Signal Process. Lett.* **2016**, *23*, 546–550. [CrossRef]
15. Qu, X.; Xie, L. An efficient convex constrained weighted least squares source localization algorithm based on TDOA measurements. *Signal Process.* **2016**, *119*, 142–152. [CrossRef]
16. Doğançay, K.ı.l. 3D Pseudolinear Target Motion Analysis From Angle Measurements. *IEEE Trans. Signal Process.* **2015**, *63*, 1570–1580. [CrossRef]
17. Jia, T.; Wang, H.; Wang, G.; Ho, K.C. Localization Using Time-Delay and Doppler Shift by Moving Monostatic Sensors. *IEEE Trans. Aerosp. Electron. Syst.* **2022**, *58*, 2560–2567. [CrossRef]
18. Jia, T.; Wang, H.; Shen, X.; Jiang, Z.; He, K. Target localization based on structured total least squares with hybrid TDOA-AOA measurements. *Signal Process.* **2018**, *143*, 211–221. [CrossRef]
19. Ho, K.C.; Wenwei, X. An accurate algebraic solution for moving source location using TDOA and FDOA measurements. *IEEE Trans. Signal Process.* **2004**, *52*, 2453–2463. [CrossRef]
20. Bishop, A.N.; Fidan, B.; Anderson, B.D.O.; Pathirana, P.N.; Dogancay, K. Optimality Analysis of Sensor-Target Geometries in Passive Localization: Part 2-Time-of-Arrival Based Localization. In Proceedings of the 2007 3rd International Conference on Intelligent Sensors, Sensor Networks and Information, Melbourne, Australia, 3–6 December 2007; pp. 13–18.
21. Zhou, C.; Huang, G.M.; Gao, J. Optimum Sensor Array for Passive Localization from Time Differences of Arrival. *Appl. Mech. Mater.* **2015**, *721*, 411–415. [CrossRef]
22. Ho, K.C.; Vicente, L.M. Sensor Allocation for Source Localization With Decoupled Range and Bearing Estimation. *IEEE Trans. Signal Process.* **2008**, *56*, 5773–5789. [CrossRef]
23. Zhong, Y.; Wu, X.; Huang, S.; Li, C.; Wu, J. Optimality Analysis of Sensor-Target Geometries for Bearing-Only Passive Localization in Three Dimensional Space. *Chin. J. Electron.* **2016**, *25*, 391–396. [CrossRef]
24. Bo, W.; Lei, X. Station arrangement strategy of TDOA/AOA location system based on genetic algorithm. *Comput. Eng. Appl.* **2009**, *45*, 219–221.
25. Sun, R.; He, Z.; Gao, L.; Bai, J. Station Layout Optimization Genetic Algorithm for Four Stations TDOA Location. *J. Phys. Conf. Ser.* **2019**, *1176*, 062008. [CrossRef]
26. YAN Qing-li, C.J.-F. Node Placement Optimization for Distributed Acoustic Source Localization System and Performance Study. *Acta Electron. Sin.* **2018**, *46*, 1186–1193.
27. Chan, Y.T.; Ho, K.C. A simple and efficient estimator for hyperbolic location. *IEEE Trans. Signal Process.* **1994**, *42*, 1905–1915. [CrossRef]
28. Hu, A.; Deng, Z.; Yang, H.; Zhang, Y.; Gao, Y.; Zhao, D. An Optimal Geometry Configuration Algorithm of Hybrid Semi-Passive Location System Based on Mayfly Optimization Algorithm. *Sensors* **2021**, *21*, 7484. [CrossRef] [PubMed]